alcohol (ca. 10 ml) was added and evaporation and cooling caused precipitation of the Reissert compound. Treatment and of the Reissert compounds (x g) dissolved in a minimum of hot acetic acid, with 40% aqueous fluoroboric acid (3.5 × x g), followed by cooling produced the hydrofluoroborate salt which was collected by filtration and either washed or recrystallized from ethanol. Reissert compounds and their salts obtained via this general procedure are reported in Table III. New compounds gave satisfactory elemental analysis data and melting points of known compounds agreed with those reported previously.

α-Deuterated Reissert Compounds. These were prepared by the following general route. The Reissert compound (2 g) was taken up in sufficient TFA to obtain a clear solution (ca. 4 ml). This solution was added dropwise to a swirled flask containing dry ether (100 ml). The solid was filtered off and ground with anhydrous sodium carbonate in a mortar and pestle. D_2O (5–10 ml) was added to obtain a thick paste which was mixed thoroughly for 5 min. The mixture was then taken up in chloroform (20 ml), the organic layer separated, and the aqueous layer washed with chloroform (2 × 10 ml). The combined organic fractions were then dried (Na_2CO_3) and evaporated to dryness, and the product was recrystallized from 1:10 benzene/cyclohexane (ca. 20–40 ml). The α-deuterated Reissert compounds were shown to have melting points and mixed melting points identical with the parent compounds.

Acknowledgments. We thank Professor W. E. McEwen for helpful discussion and the S.R.C. for financial support (to A.D.P.).

References and Notes

(1) (a) Part XII: S. O. Chua, M. J. Cook, and A. R. Katritzky, *J. Chem. Soc. B*, 2350 (1971); (b) part XIII: G. Blanchi, A. J. Boulton, I. J. Fletcher, and A. R. Katritzky, *ibid.*, 2355 (1971).
(2) For reviews, see (a) W. E. McEwen and R. L. Cobb, *Chem. Rev.*, **55**, 511 (1955); (b) F. D. Popp, *Adv. Heterocycl. Chem.*, **9**, 1 (1968).
(3) See, e.g., F. D. Popp and W. Blount, *J. Org. Chem.*, **27**, 297 (1962).
(4) R. L. Cobb and W. E. McEwen, *J. Am. Chem. Soc.*, **77**, 5042 (1955).
(5) J. W. Davis, Jr., *J. Org. Chem.*, **25**, 376 (1960).
(6) W. E. McEwen, I. C. Mineo, and Y. H. Shen, *J. Am. Chem. Soc.*, **93**, 4479 (1971).
(7) For reviews, see (a) A. R. Katritzky and J. M. Lagowski, *Adv. Heterocycl. Chem.*, **2**, 27 (1963); (b) J. Elguero, C. Marzin, A. R. Katritzky, and P. Linda, "The Tautomerism of Heterocycles", Academic Press, New York, N.Y., 1976.
(8) See ref 7b, pp 431–433.
(9) W. E. McEwen, M. A. Calabro, I. C. Mineo, and I. C. Wang, *J. Am. Chem. Soc.*, **95**, 2392 (1973).
(10) A. J. Birch, A. H. Jackson, and P. V. R. Shannon, *Tetrahedron Lett.*, 4789 (1972).
(11) J. M. Bobbitt, J. M. Kiely, K. L. Khanna, and R. Ebermann, *J. Org. Chem.*, **30**, 2247 (1965); J. M. Bobbitt and J. C. Sih, *ibid.*, **33**, 856 (1968).
(12) A. D. Page, Ph.D. Thesis, University of East Anglia, 1976.
(13) F. D. Popp, K. T. Potts, and R. Armbruster, *Org. Mass Spectrom.*, **3**, 1075 (1970).
(14) A. Bischler and B. Napieralski, *Chem. Ber.*, **26**, 1903 (1893).
(15) W. M. Whaley and M. Meadow, *J. Chem. Soc.*, 1067 (1953).
(16) Moreover, no authenticated examples of the isolation of a nonthermodynamically stable imino form are known.[7]
(17) Examination of the actual spectra as recorded in the Ph.D. Thesis of I. C. Wang, University of Massachusetts, 1971, supports this view.

Kinetics and Thermodynamics of Intermolecular Saturated Amine Excimers

Arthur M. Halpern,*[1] Pierre Ravinet,[2] and Ronald J. Sternfels[3]

Contribution from the Photochemistry and Spectroscopy Laboratory, Department of Chemistry, Northeastern University, Boston, Massachusetts 02115.
Received April 30, 1976

Abstract: The rate constants and activation parameters pertaining to excimer formation in 1-azabicyclo[2.2.2]octane (ABCO) and 1-azaadamantane (1-AA) have been measured in n-hexane solution utilizing fluorescence decay data. These excimers are characterized spectroscopically by broad, very red-shifted emission bands (λ_{max} 375 and 395 nm, respectively). The formation rate constants are diffusion controlled and have been analyzed without the need to consider the "transient term". These excimers are rather tightly bound having ΔH values of −11.6 and −10.2 kcal/mol, respectively. In addition, the dissociation rate constant preexponential factors are typically large, with ΔS values of ca. 19 and 17 eu, respectively. The methodology of determining binding energies using the steady-state method vis-a-vis kinetic procedures is discussed; the former technique provides lower limits of $|\Delta H|$ values. For ABCO, the excimer relaxation rate constant, k_D, was found to be slightly temperature dependent ($W_D \sim 1.4$ kcal/mol), and an analysis of the temperature dependence of the excimer fluorescence quantum intensity revealed that it is the nonradiative portion of k_D which varies with temperature. The ABCO excimer is weakly quenched by ground-state amine ($k_{QD} = 7.2 \times 10^7$ M^{-1} s^{-1}). The photophysical properties of nonexcimer-forming amines are compared with ABCO and 1-AA, and an attempt is made to rationalize the stability of these excimers within simple exciton and charge resonance models. Neither approach appears to be adequate in accounting for the observed binding energies or in explaining the structural specificity in excimer formation in saturated amines. The structure of the excimer is discussed and configurations are proposed: head-to-head (N—N) and C–N bond antiparallel to C–N bond. The head-to-tail arrangement is excluded because 4-Me-ABCO also undergoes excimer formation and possesses similar thermodynamic properties. The photochemistry of ABCO and triethylamine (in n-hexane) solution is also discussed.

Introduction

The association between an electronically excited molecule and its ground-state counterpart (i.e., excimer formation) is a well-known phenomenon which has been extensively studied, both experimentally and theoretically, for about 20 years.[4-7] Until rather recently, however, investigations of organic molecular excimers and their formation, deactivation, stability, etc. have been confined to aromatic or heteroaromatic molecules.[7,8] Studies of excimer formation in some nonaromatic compounds, i.e., saturated tertiary amines, have been described recently.[9,10] It thus appears that the presence of the π-electronic system characteristic of aromatic molecules is not an essential criterion for the stabilization of excimers in organic molecules.[11] Thus the nonbonding electron pair in a saturated amine, when properly oriented in certain aliphatic systems can be very important in effecting excimer stabilization both *inter*molecularly and intramolecularly.[12] It is the purpose of this

paper to present the results of detailed kinetic and thermodynamic studies of some saturated amine excimers, to suggest possible geometries of these interesting systems, and to speculate about the nature of the binding forces in these excimers.

Although the photophysical properties of a large number of saturated amines have been investigated in this laboratory under widely varying experimental conditions (i.e., vapor phase, solvent media of differing polarity, temperature, etc.), only three amines have been unequivocally demonstrated to undergo intermolecular excimer formation. These compounds are: 1-azabicyclo[2.2.2]octane (ABCO), 4-Me-ABCO, and

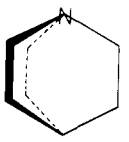

ABCO

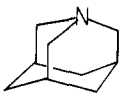

1AA

1-azaadamantane (1-AA). The vapor pressures of ABCO and 4-Me-ABCO are sufficiently high under ambient conditions so that excimer formation is observable in the vapor phase for these amines; for example, the vapor pressure of ABCO is about 2 Torr (ca. 1×10^{-4} M) at 23 °C and is large enough to allow pressure dependent studies to be carried out. The formation and dissociation kinetics of the ABCO vapor phase excimer have been reported recently.[10] The vapor pressure of 4-Me-ABCO is about 3 Torr under ambient conditions.

Results and Discussion

Absorption Spectra. Unless otherwise indicated, all studies were carried out using *n*-hexane as the solvent medium. First the electronic absorption spectra of the amines will be summarized. Assignments of the electronic absorption spectra of the trialkylamines have been suggested only in the vapor phase wherein the upper states are believe to be Rydberg in nature.[13] Thus, the lowest lying excited state is assigned as (n,3s) and the next higher two states as (n,3p) and (n,4p). Although it is recognized that states arising from valence shell conjugate orbitals (i.e., σ^* orbitals) are important, the location of these V ← N states in the trialkylamines has not been conclusively identified.[13,14]

The vapor phase absorption spectra of each of the excimer-forming cage amines depicted above are characterized by highly structured vibronic features.[15,16] Significantly, these vibrational patterns are completely absent in the spectra obtained in an *n*-hexane medium. This phenomenon can be interpreted as being a consequence of the Rydberg nature of the excited states.[13] It is probably incorrect, however, to assume that in condensed media, the Rydberg states become primarily "washed out" and replaced by the valence shell states. In any event, assuming for the moment that the "integrity" (and/or importance) of the Rydberg states is diminished in the condensed phase relative to the vapor state, one is led to the conclusion that the electronic character (i.e., the degree of Rydberg/valence shell importance) of the upper state(s) is not crucial to excimer formation in the amines. This follows from the fact that the energetics and kinetics of excimer formation in ABCO are not very different in the vapor phase vis-a-vis *n*-hexane solution.[10]

The absorption spectra of the trialkylamines in *n*-hexane solution (including the cage amines discussed here) are rather undistinguished, consisting of a moderately intense maximum in the 200-nm region with tailing to lower energies, out to ca. 255 nm. In certain amines, e.g., ABCO, an inflexion in the 230-nm region can be discerned, and using the more information-laden vapor phase spectra as a guide, the transition possessing the maximum near 200 nm can most likely be correlated with the 3p ← n transition ($S_2 \leftarrow S_0$), and the long wavelength shoulder (or tail) can be associated accordingly with the 3s ← n transition ($S_1 \leftarrow S_0$). It should be realized that the presence of the valence shell conjugate as a continuum overlapping these (proposed) Rydberg excitations cannot be ignored. The detailed vapor phase absorption spectra of ABCO have been reported elsewhere,[15] and the 3p ← n ($S_2 \leftarrow S_0$) spectrum of 1-AA has been published.[16] The absorption spectrum of ABCO in *n*-hexane is shown in Figure 1, and as mentioned above, the rich vibronic structure which characterizes the vapor state spectra is completely absent. Thus this spectrum resembles those of other saturated amines.[17] It is important to note that the cage amines reported in this paper, as well as many other monocyclic and acyclic amines, obey Beer's Law in hydrocarbon solvents up to at least ca. 10^{-1} M). This seems to preclude the possibility of (discrete) ground-state interactions between these saturated amine solutes.

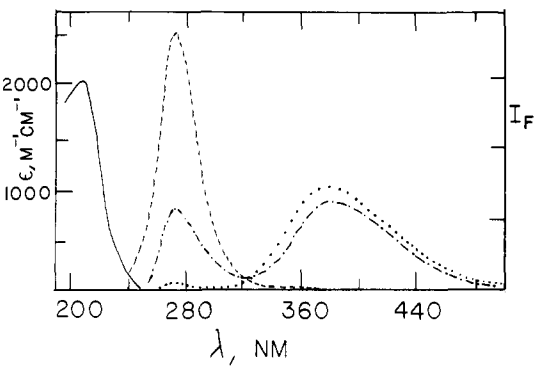

Figure 1. Spectra of ABCO in *n*-hexane solution at 23 °C: (—) absorption spectrum; (- - - -) emission spectrum 2.0×10^{-4}; (-·-) 2.0×10^{-3} M; (· · · · ·) 2.0×10^{-2} M. Emission spectra are uncorrected and are obtained with λ_{exc} of 238 nm.

Fluorescence Spectra. In the vapor phase, both ABCO and 4-Me-ABCO are characterized by rather highly structured fluorescence spectra (if the excitation energies are kept below ca. 4000 cm^{-1} of the respective $S_1 \leftarrow S_0$ energies (and/or vibrational relaxation is ensured by the presence of a buffer gas). ABCO's fluorescence spectrum has been described elsewhere.[10,18] In *n*-hexane solution, the fluorescence spectra, like the absorption spectra of the three cage amines reported here are structureless, having maxima in the 270–286 nm region. Some pertinent data concerning the absorption and fluorescence spectra of ABCO, 4-Me-ABCO, and 1-AA are summarized in Table I. These data show that in refluorescence, there is no discernible shift in the solution phase maxima when compared with the (estimated) maxima of the respective Franck-Condon envelopes of the vapor phase spectra. It should also be noted that the transition energies of ABCO and 4-Me-ABCO are very similar whereas 1-AA absorbs (and emits) considerably to the red, presumably as a consequence of the higher degree of alkylation (and hyperconjugation) of the latter amine.[19] The lack of a dramatic solvation effect on the fluorescence spectra of these amines is somewhat puzzling in view of the presumed Rydberg nature of their upper states. On the other hand, it has been suggested that the fluorescence from simple acyclic amines originates from an underlying valence shell state.[20] This point is not easily disposed of, because in the cage amines, the correspondence between the fluorescence and $S_1 \leftarrow S_0$ absorption spectra in the vapor phase (i.e., the coincidence of the 0-0 bands, correlation of vibrational progression frequencies, etc.) would seem to support the idea that fluorescence originates in fact from the (n_N,3s) Rydberg state.

It is interesting to compare the energies of the fluorescence

Table I. Absorption and Fluorescence Data for the Cage Amines in the Vapor Phase and in *n*-Hexane Solution at 23 °C

	Absorption[a]					Fluorescence[a]			
	Vapor[b]			Solution		Vapor		Solution	
Amine	$S_1 \leftarrow S_0$	$S_2 \leftarrow S_0$	$S_3 \leftarrow S_0$	λ_{max} (ϵ_{max})[c]	ϵ (238 nm)[c]	Monomer	Excimer	Monomer	Excimer
ABCO	255.9	228.0	188.3	206 (1980)	247	271[d]	375	272.5	375
4-MA	252.3	227.8	*e*	207 (2330)	222	268[d]	375	270	375
1-AA	265.5	236.7	195.8	211 (1970)	252	289[d]	*f*	286.5	395

[a] Wavelength values in nm. [b] 0–0 bands. [c] M^{-1} cm^{-1}. [d] Emission is structured; apparent λ_{max} of Franck-Condon envelope. [e] The origin is not located with certainty. [f] Excimer emission is not observed in the vapor phase at 23 °C.

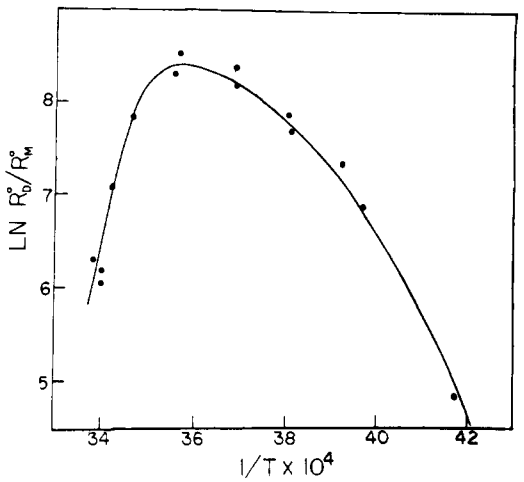

Figure 2. Plot of ln $[I_{fD}/I_{fM}]$ vs. $1/T$ for ABCO in *n*-hexane; λ_{exc} is 238 nm.

maxima of ABCO (or 4-Me-ABCO) and an acyclic amine containing a similar number of alkyl groups, e.g., triethylamine. λ_{max} (fluorescence) for triethylamine lies about 10 nm to the red of ABCO, i.e., at about 282 nm (see Table I). This is probably due to the fact that whereas emission from the acyclic amine takes plce from a planar (or nearly planar) equilibrated excited state, the three ethylene bridges constrain ABCO from achieving a planar upper state, and this molecule will exhibit, accordingly, less of a geometry change-inducing Stokes shift that flexible triethylamine. These structural and spectroscopic distinctions between rigid and nonrigid amines bear interesting consequences vis-a-vis the temperature dependence of fluorescence intensity in these types of amines.[21]

The fluorescence spectra of all nonrigid (tertiary) amines examined to date are concentration independent, although many of these amines undergo self-quenching. Many rigid amines, such as 1-azabicyclo[3.3.3]undecane and 1,4-diazabicyclo[2.2.2]octane (DABCO), also exhibit concentration independent fluorescence spectra. On the other hand, the spectra of ABCO, 4-Me-ABCO, and 1-AA are all concentration dependent. Thus in dilute solutions (ca. 10^{-5}–10^{-4} M in *n*-hexane), these amines fluoresce in the ultraviolet region and, as such, resemble typical saturated amines (except for a small blue shift, vide supra). As the concentration of these amines is increased, a significantly red-shifted, broad, structureless emission band appears and gains prominence with increasing concentration. At about 10^{-2} M, the fluorescence spectra of these cage amines are almost fully characterized by the respective long wavelength bands, and the fluorescence is perceived by the eye as a bright violet color. This behavior is also illustrated in Figure 1 for ABCO. The fluorescence maxima of the long wavelength bands of the cage amines are summarized in Table I.

This long wavelength emission band has been assigned as excimer fluorescence on the basis of its temporal, thermal, and concentration dependence. The short wavelength fluorescence band (the only band observable in very dilute solutions) will be referred to as *monomer* emission. It should be noted that the series of emission spectra shown in Figure 1 for ABCO does not exhibit the usual isoemissive point which characterizes most aromatic excimer systems. The failure of ABCO to manifest an isoemissive point is a consequence of excimer quenching by ground-state molecules and will be discussed in more detail below.

First, the temperature dependence of the monomer and excimer bands will be discussed, and the results of kinetic studies will be presented subsequently. It will be convenient, however, to introduce at this point the kinetic scheme (Scheme I) which will be applied to the saturated amine excimer systems. The denotation of rate constants follows that of Birks.[5] Monomer and excimer decay constants are defined as follows:

Scheme I

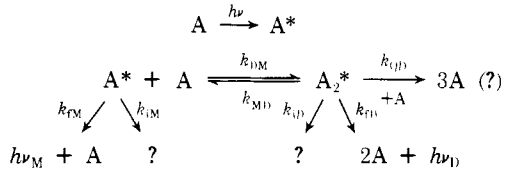

$$k_M = k_{iM} + k_{fM}$$

$$k_D = k_{iD} + k_{fD} + k_{QD}[C]$$

where k_{iM} and k_{fM}, k_{iD} and k_{fD} are the nonradiative and radiative rate constants for the monomer and excimer, respectively. One additional step has been added to the usual monomer/excimer system, namely, the quenching of the excimer by ground-state amine (rate constant k_{QD}). Under conditions of steady-state excitation, the well-known relation for the ratio of excimer to monomer fluorescence intensities is:

$$\frac{I_{fD}}{I_{fM}} = \left(\frac{k_{DM}[C]}{(k_D + k_{MD})}\right)\left(\frac{k_{fD}}{k_{fM}}\right) \quad (1)$$

where k_{DM} and k_{MD} are the excimer formation and dissociation rate constants, respectively; k_M and k_D are the monomer and excimer composite relaxation rate constants *irrespective* of the coupling with each other; k_D is concentration dependent as a consequence of the quenching process mentioned above.

In eq 1, k_{DM} and k_{MD} are usually regarded as being the only

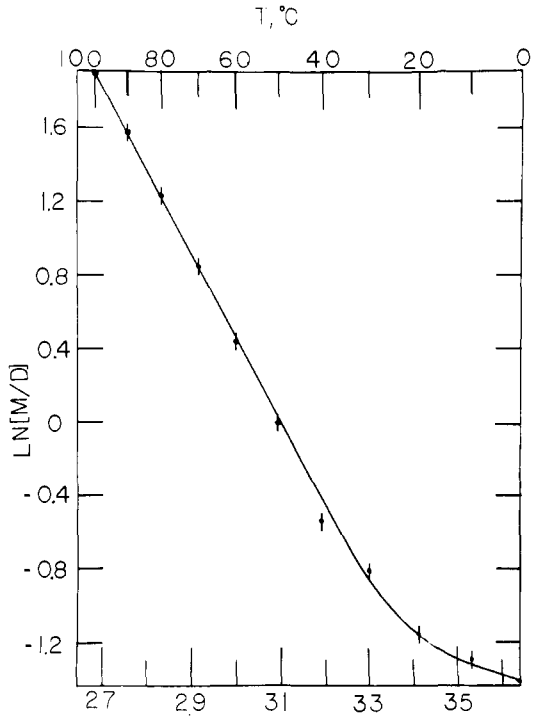

Figure 3. Plot of ln $[I_{fD}/I_{fM}]$ vs. $1/T$ for 1-AA in *n*-hexane (in the high-temperature region); λ_{exc} is 238 nm.

(strongly) temperature-dependent rate constants.[22] If the temperature is high enough so that the excimer dissociation rate exceeds the intrinsic (i.e., radiative and nonradiative) depletion rate of the excimer, $k_{MD} > k_D$, and an Arrhenius plot of the ratio of excimer to monomer fluorescence intensities can be used to obtain approximate values of the enthalpy and entropy of excimer formation.[23] In the "low-temperature region", $k_{MD} < k_D$, and an Arrhenius plot of eq 1 can provide an estimate of the activation energy to excimer formation (i.e., W_{DM}) which can, in some cases, be correlated with the temperature coefficient of the solvent viscosity.[4] When plotted over a wide temperature range, ln (I_{fD}/I_{fM}) vs. $1/T$ is distinctly curved and actually goes through a maximum; i.e., excimer fluorescence intensity is surpressed both at very high and very low temperatures.[24] Thus it should be realized that, in principle, the excimer formation enthalpy (ΔH) and activation barrier (W_{DM}) can be obtained only in the limits of very high and low temperatures, respectively. Thus the ability of these steady-state data to provide ΔH and W_{DM} hinges on how far the experimental temperature range is from the maximum in such an Arrhenius plot and also depends upon the relative magnitudes of k_{MD} and k_D for a particular excimer system. Discrepancies between enthalpy values obtained from steady-state data (as outlined above) and kinetic data (from $\Delta H = W_{DM} - W_{MD}$) have been noted before.[24,25] An Arrhenius plot of the ratio of excimer to monomer fluorescence intensities is shown in Figure 2 in which the temperature range is wide enough to enable the maximum (at T_{max}) to be included. A similar plot for 1-AA over a narrower temperature range is illustrated in Figure 3. It appears to be linear above ca. 40 °C and furnishes an "apparent" ΔH value of ca. −8.9 kcal/mol which compares with −10.2 kcal/mol obtained from kinetic measurements. An expression for T_{max} can be obtained from eq 1, assuming that k_D, k_{fD}, and k_{fM} are independent of temperature; k_{MD} and k_{DM} are represented as Arrhenius rate constants:

$$k_{DM} = A_{DM} \exp(-W_{DM}/RT)$$

$$k_{MD} = A_{MD} \exp(-W_{MD}/RT)$$

where the A's and W's are the respective activation parameters for excimer formation and dissociation.[4] Although knowledge of the value of T_{max} obtained experimentally is not very useful in determining any of the rate or activation parameters per se, eq 1a can be used to check the internal consistency of the

$$T_{max} = \frac{W_{MD}}{R \ln [(A_{MD}/k_D)(W_{MD}/W_{DM} - 1)]} \quad (1a)$$

various activation parameters once determined by other, more direct means. Experimentally measured T_{max} values for ABCO and 1-AA are 8 and −10 °C, respectively, and are favorably compared with the calculated values of 14 and −13 °C for these systems. It should be noted that the slight temperature dependence observed for k_D in the ABCO excimer vide infra renders eq 1a approximate; nevertheless, the decent agreement between the measured and calculated T_{max} values implies that the approximation is reasonably good in these cases.

Kinetic Analysis

One of the goals in studying excimer formation is to elucidate all of the seven rate constants (and their activation parameters) which pertain to the excimer/monomer scheme outlined above. To achieve this end, one pursues the basic methodology of obtaining and analyzing both the monomer and excimer decay curves as a function both of temperature and concentration. Absolute quantum yield determinations are, of course, necessary in order to partition the monomer and excimer relaxation rate constants (k_M and k_D) into their respective radiative and nonradiative components.

Solving the appropriate coupled differential equations involving the disappearance rates of excited monomer and excimer results in the following well-known relations for the time dependencies of monomer and excimer fluorescence intensities, respectively:

$$I_{fM}(t) \propto \exp(-\lambda_1 t) + A \exp(-\lambda_2 t) \quad (2)$$

$$I_{fD}(t) \propto \exp(-\lambda_1 t) - \exp(-\lambda_2 t) \quad (3)$$

where

$$2\lambda_{1,2} = X + Y \mp \sqrt{(X - Y)^2 + 4k_{MD}k_{DM}C} \quad (4)$$

C is the concentration (in M) of the amine, and X, Y, and A are defined as:

$$X = k_M + k_{DM}C \quad (5)$$

$$Y = k_D + k_{MD} + k_{QD}C \quad (6)$$

$$A = (X - \lambda_2)/(\lambda_2 - X) \quad (7)$$

Equations 2 and 3 hold for δ pulse excitation of ground-state amine.

Thus it is expected that over certain temperature and concentration ranges, the monomer fluorescence intensity should exhibit a double exponential decay curve. The ratio of the amplitudes of the short to the long components of the monomer decay curve is, then, equal to A. The excimer decay curve is accordingly expected to appear as the difference of two components having equal amplitudes. This decay curve is characterized by the well-known build-up time to maximum intensity which is then followed by an exponential decay (having a slope equal to $-\lambda_1$). Representative decay curves for 1-AA monomer and excimer are shown in Figures 4 and 5, respectively. Analogous decay curves for the ABCO system have been published elsewhere.[9]

Using the following relation for the build-up time, t_{max}:

$$t_{max} = \ln (\lambda_2/\lambda_1)/(\lambda_2 - \lambda_1)$$

it is possible to determine λ_2 from an excimer decay curve (i.e., knowing λ_1) and t_{max}. In practice, however, it appears that this

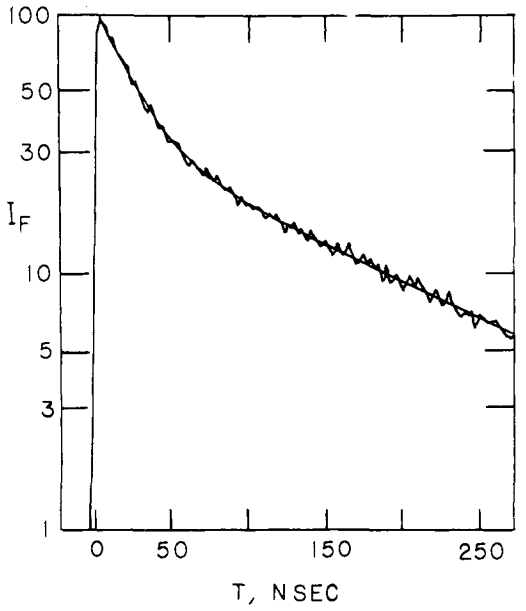

Figure 4. Decay curve of monomer fluorescence of 1-AA (isolated with a 2876 Å interference filter) at 40 °C. Concentration is 1.0×10^{-3} M; λ_{exc} is 230 nm. The continuous line is the convoluted decay curve.

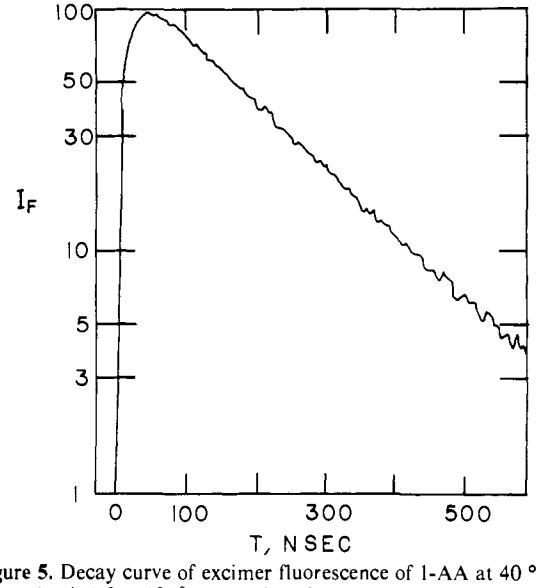

Figure 5. Decay curve of excimer fluorescence of 1-AA at 40 °C. Concentration is 1.0×10^{-3} M; λ_{exc} is 230 nm.

is not a precise way of measuring λ_2 because of the inherent error in determining t_{max} and also the insensitivity of t_{max} with respect to λ_2.

At a fixed concentration and temperature, all directly measurable kinetic information can be represented by λ_1, λ_2, and A. In principle, these three parameters can be obtained by a careful analysis of just a monomer decay curve, i.e., the two time constants and their relative amplitudes. However, under certain conditions (of concentration and temperature) it is more precise to determine λ_1 directly from an excimer decay curve and to use this value to measure λ_2 and A by a convolution-and-compare analysis of a monomer decay curve.[18] In other cases where both λ_1, λ_2 as well as A can be obtained directly from a monomer decay curve, λ_1 derived from the excimer decay curve was used as an internal check of this parameter. Agreement was always found to be satisfactory. However, it appeared that slight spectroscopic "contamination" of the excimer decay curve by monomer fluorescence (e.g., at very low concentrations and/or high temperatures) caused some discrepancy between λ_1 values obtained from an excimer decay curve vis-a-vis the respective monomer decay curve.

It is interesting to consider what the limiting values of λ_1 and λ_2 are as C approaches zero. It is obvious from eq 4 that, with respect to values of λ_1 and λ_2 calculated for finite concentrations of amine, it is irrelevant as to whether the first term under the square root is expressed as $(X - Y)^2$ or $(Y - X)^2$. In fact, it is the latter form which is usually indicated.[4,5] The *limits*, however, which are determined for λ_1 and λ_2 as $C \rightarrow 0$ depend on how this term is represented. For example, from eq 4 it follows that

$$\lim_{C \rightarrow 0} \lambda_1 = k_D + k_{MD} \tag{8}$$

and

$$\lim_{C \rightarrow 0} \lambda_2 = k_M \tag{9}$$

yet if $(Y - X)^2$ is used, these limits are switched, and

$$\begin{aligned} \lambda_1 &\rightarrow k_M \\ \lambda_2 &\rightarrow k_D + k_{MD} \end{aligned} \tag{10}$$

as $C \rightarrow 0$.

The correct set of limits which applies to an excimer system depends both on the nature of the monomer and excimer and also on the temperature of the system. In other words, if $k_M > k_D + k_{MD}$ limits 8 and 9 are valid; if $k_M < k_D + k_{MD}$, then limits 10 apply. At ambient temperatures, limits 10 pertain to the pyrene excimer, while limits 8 and 9 describe the saturated amine excimers described in this paper. Because the excimer dissociation rate constant, k_{MD}, is much more strongly temperature dependent than k_M and k_D,[26] there exists a temperature which is characteristic of an excimer system above which limits 10 apply and below which limits 8 and 9 apply. Clearly this "inversion" temperature (T') depends not only upon the formation enthalpy of the excimer (which, in turn, depends largely on W_{MD}[27]), but also on the relative values of k_D and k_M. This latter condition is determined by the magnitudes of the radiative and nonradiative transition probabilities of the monomer vis-a-vis those of the excimer.

It is important to realize that at T', the excimer system is nearly in state of dynamic equilibrium. In fact, at temperatures *above* this point (in the so-called high-temperature limit), the nonexponentiality of the monomer and excimer decay curves disappears, and both species appear to decay with a common decay constant.[5,6] The utilization of kinetic data obtained in this high-temperature region will be discussed below.

In general direct plots of λ_1 and λ_2 vs. concentration (at a fixed temperature which is $<T'$) are not very useful. Both plots are curved, having limiting slopes as follows:

$$\left(\frac{\partial \lambda_1}{\partial C}\right)_{C \rightarrow 0} = k_{DM}\left(\frac{k_{MD}}{k_D + k_{MD} - k_M}\right) + k_{QD} \tag{11}$$

and

$$\left(\frac{\partial \lambda_2}{\partial C}\right)_{C \rightarrow 0} = k_{DM}\left(1 - \frac{k_{MD}}{k_D + k_{MD} - k_M}\right) \tag{12}$$

The same experimental conditions and molecular properties which determine the proper identification of the λ_1 and λ_2 intercepts [i.e., (8) and (9), or (10)] also govern the assignment of the limiting slopes of the $\lambda_{1,2}$ vs. C plots. For the saturated amine excimers, and below T', conditions 11 and 12 apply. Plots of λ_1 vs. C for the 1-AA excimer system at 20 and 30 °C are shown in Figure 6. It is clear from this plot that the limiting slopes are negative. The error bars in the λ_1 values are typical and reflect the fact that λ_1 was obtained both from monomer

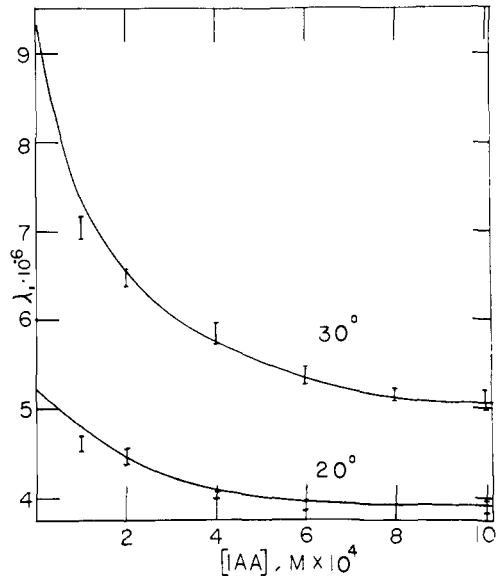

Figure 6. λ_1 plotted vs. concentration for 1-AA in *n*-hexane at 20 and 30 °C. The solid line is obtained from eq 4 and from the rate constants listed in Table II.

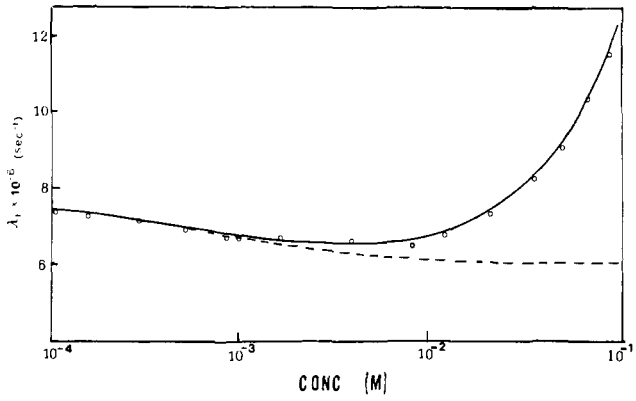

Figure 7. (○) Experimental values of λ_1 for ABCO in *n*-hexane at 25 °C plotted as a function of log concentration. (—) λ_1 calculated from eq 4, using a value of $k_{QD} = 7.2 \times 10^7$ M^{-1} s^{-1} and other rate constants consistent with the rate constants and activation parameters listed in Tables III and IV. (- - - -) λ_1 calculated from eq 4 but with $k_{QD} = 0$.

and excimer decay curves. Moreover, the negative slope observed for these plots indicates that $k_{QD} \ll k_{DM}$ [see (11)].

It can be seen from (11) an (12) that at T', the limiting slopes of these plots become indeterminate. Also, as the temperature approaches T', $\lambda_1 \rightarrow \lambda_2$ in the limit of $C \rightarrow 0$. Experimentally, these conditions (i.e., T near T' and low C) have the effect of imposing extraordinarily large errors on values of λ_1 and λ_2 as determined from monomer and excimer decay curves. For 1-AA and ABCO this region is ca. $<10^{-4}$ M and 40–50 °C.

It is useful to consider the behavior of the λ_1 and λ_2 vs. C plots at higher concentrations. In the high concentration limit, these plots become linear and have the following slopes:

$$\left(\frac{\partial \lambda_1}{\partial C}\right)_{1/C \rightarrow 0} = k_{QD}$$

and

$$\left(\frac{\partial \lambda_2}{\partial C}\right)_{1/C \rightarrow 0} = k_{DM}$$

The *extrapolated* intercept of the linear portion of the λ_1 vs. C plot is equal to k_D. For ABCO, the λ_1 vs. C plots approach linearity above ca. 5×10^{-3} M. This feature is helpful not only in obtaining values of the excimer quenching constant, k_{QD}, but also in providing a means for measuring k_D. In practice, k_D was usually evaluated by an alternate method (to be described below); nevertheless, k_D obtained from the extrapolated intercept of the λ_1 vs. C plot was used as an internal check. One of the problems associated with this method is that k_{QD} seems, in general, to be very small, and its measurement required rather high amine concentrations. In fact, for 1-AA, k_{QD} appears to be considerably smaller than in the case of the ABCO excimer, and λ_1 vs. C plots did not begin to curve upward until about 10^{-2} M. The limited amount of this amine available for our study precluded carrying out reliable measurements above ca. 2×10^{-2} M.

Presumably, any reasonable efficient quenching process involving only the excimer could be studied in the way described above in order to obtain values of k_D. For some excimer (or exciplex) systems, this might prove to be a more convenient method of determining this rate constant. The necessity of including k_{QD} in the ABCO excimer kinetic scheme is best illustrated in Figure 7 in which both experimental and calculated values of λ_1 are plotted vs. C. The omission of k_{QD} from k_D (and thus from eq 4) results in the computed values of λ_1 represented by the dashed line in Figure 7. The value of k_{QD} used in the solid line calculation was obtained from the procedure described below.

Determination of Rate Constants

At a given temperature, the monomer/excimer rate constants k_M, k_D, k_{MD}, k_{DM} (and for ABCO, k_{QD}) were directly determined from an analysis of the concentration dependence of λ_1, λ_2, and A. For each amine studied and at given temperature there exists a range of concentrations over which the *simultaneous* measurement of these three kinetic parameters can be measured with high enough precision to be useful in the analysis described below. Thus, for 1-AA and ABCO, this concentration range (at ambient temperatures) was found to be ca. 10^{-4} M to ca. 10^{-3} M. At higher and lower temperatures, this range becomes somewhat smaller.

I. X is determined as follows:

$$X = \frac{A\lambda_1 + \lambda_2}{(1 + A)} \tag{13}$$

and then plotted vs. C. The slope and intercept of this plot are k_{DM} and k_M, respectively. The ability to measure meaningful X values begins to fail as A becomes very large (i.e., at low concentrations and/or at high temperatures).

II. The quantity $\lambda_1 + \lambda_2$ is plotted vs. C furnishing as the slope, $k_{DM} + k_{QD}$, and as the intercept, $k_M + k_D + k_{MD}$. Because the value of k_{QD} is very small (as compared with k_{DM}) for both ABCO and 1-AA, the slopes of plots I and II were found to be experimentally indistinguishable. The difference in the intercepts between these two plots gives the sum: $k_D + k_{MD}$. Examples of plots of X and $\lambda_1 + \lambda_2$ (portrayed on the same axes) obtained at 30 °C are shown in Figures 8 and 9 for 1-AA and ABCO, respectively.

III. k_{MD} is elucidated by plotting

$$(X - \lambda_1)(\lambda_2 - X) \tag{14}$$

vs. C. The slope of this plot is simply $k_{MD}k_{DM}$, and the intercept is 0, giving somewhat higher precision to the slope measurement considering the presence of inherent scatter in the points. k_{MD} is then obtained by using the value of k_{DM} measured from the slope of (13). The calculation of (14) directly from the monomer and excimer decay curve parameters fails when X [measured from (13)] approaches λ_2 (i.e., at high concentrations and/or low temperatures). Plots of (14) vs. C are depicted in Figures 10 and 11 for 1-AA and ABCO, respectively, at 30 °C.

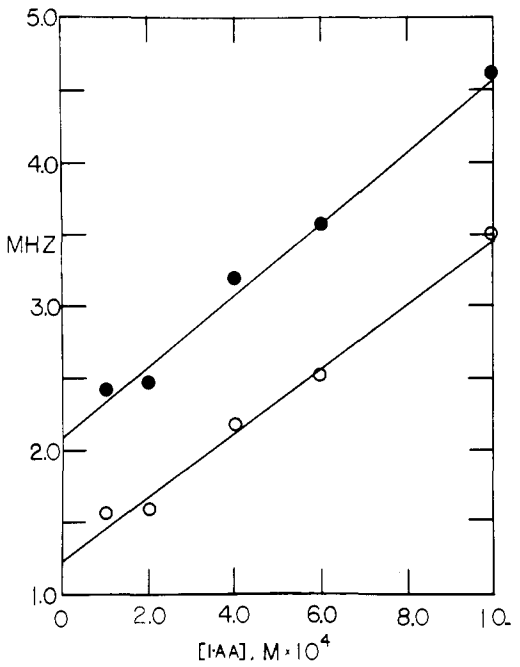

Figure 8. (●) Plot of $\lambda_1 + \lambda_2$ vs. concentration for 1-AA in *n*-hexane at 30 °C; (○) plot of X (see eq 13) vs. concentration for 1-AA in *n*-hexane at 30 °C.

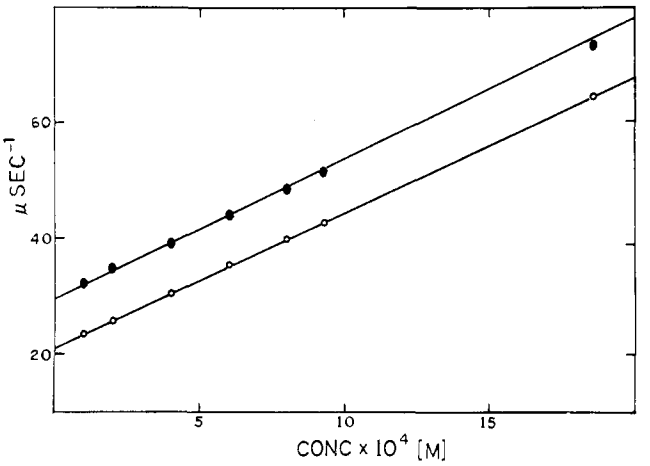

Figure 9. (●) Plot of $\lambda_1 + \lambda_2$ vs. concentration for ABCO in *n*-hexane at 30 °C. (○) Plot of X (see eq 13) vs. concentration for ABCO in *n*-hexane at 30 °C.

IV. k_D is then determined by subtracting k_{MD} from $k_D + k_{MD}$ [see (II)]. For the ABCO excimer, it was found that k_D could be obtained more accurately from V, as follows:

V. A plot of λ_1 vs. C approaches linearity at high concentrations of ABCO (i.e., above ca. 5×10^{-3} M). The limiting slope of this plot is equal to k_{QD}, and the extrapolated intercept of this plot is k_D. This technique for obtaining k_{QD} and k_D for the 1-AA excimer system was not exploited as a result of the scarcity of the amine.

Using the approach outlined in procedures I–V above, the rate constants for the 1-AA and ABCO monomer/excimer systems were obtained at several temperatures. It should be mentioned that the technique of plotting the product $\lambda_1 \times \lambda_2$ vs. C was also considered as a method of obtaining kinetic information. One would expect such plots to be quadratic (for large enough values of k_{QD}). These plots were, in fact, occasionally curved both for the 1-AA and ABCO systems despite the fact that k_{QD} is considerably smaller than k_{DM} for both amines.[28] It should be emphasized at this point that the ability

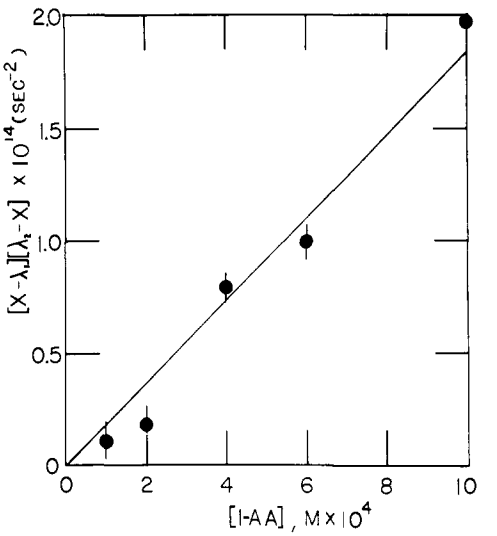

Figure 10. Plot of $[X - \lambda_1][\lambda_2 - X]$ vs. concentration for 1-AA in *n*-hexane at 30 °C.

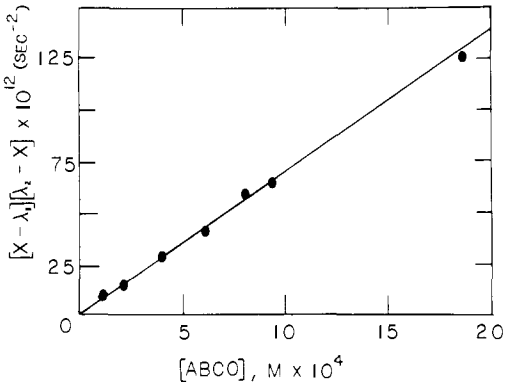

Figure 11. Plot of $[X - \lambda_1][\lambda_2 - X]$ vs. concentration for ABCO in *n*-hexane at 30 °C.

to obtain reliable and consistent values of the four rate constants for the amine excimers (five, in the case of ABCO) requires very precise *and* accurate values of λ_1, λ_2, and A under isothermal conditions (see Experimental Section).

As a check of the consistency of the rate constants determined both for 1-AA and ABCO (at the various temperatures studied), plots of λ_1, λ_2, and A vs. C were obtained via eq 3 and 4 and compared with plots of the respective experimental data. In all cases, these comparisons were considered to be satisfactory (e.g., see Figure 6). For both amines however, it was found that deviations from the calculated values of λ_1, λ_2, and A were encountered at very low amine concentrations (below ca. 10^{-4} M) especially as the temperature approached T' (vide supra).

The monomer and excimer rate constants, k_M and k_D, were partitioned into their respective radiative and nonradiative parts by measuring the intrinsic quantum yields of the monomer and excimer: q_{fM} and q_{fD}. These measurements were carried out at one temperature only (30 °C) and were corrected for excimer formation and dissociation (see Experimental Section). The results of the kinetic analysis of the 1-AA and ABCO excimer systems at various temperatures are summarized in Tables II and III, respectively. Table III also contains the data concerning the vapor phase ABCO excimer.

It is interesting to compare the radiative rate constants, k_{fM}, of these excimer-forming amines with those of other tertiary amines. For such nonrigid amines as triethylamine, dimethylethylamine, and *N*-methylpiperidine, the radiative rate

Table II. Rate Constants and Fluorescence Quantum Yields Pertaining to the 1-AA Excimer System (*n*-Hexane Solution)

	Temperature, °C					
Rate constant (units)	2	10	20	30	40	50
k_M (10^7 Hz)	1.3	1.3	1.3	1.2	1.2	1.3
k_{DM} (10^{10} M^{-1} Hz)	1.8	1.9	2.1	2.2	2.3	
k_{MD} (10^6 Hz)	1.0	2.1	3.1	7.6	13.0	
k_D (10^6 Hz)	1.8	1.5	1.7	1.7	2.1	2.0
q_{fM} (abs)				0.09		
k_{fM} (10^6 Hz)				1.1		
k_{iM} (10^7 Hz)				1.1		
q_{fD} (abs)				0.17		
k_{fD} (10^5 Hz)				2.9		
k_{iD} (10^6 Hz)				1.4		

Table III. Rate Constants and Fluorescence Quantum Yields Pertaining to the ABCO Excimer System (*n*-Hexane Solution)

	Temperature, °C								
Rate constant (units)	−10	0	10	20	26[a]	30	40	60	90
k_M (10^7 Hz)	2.1	2.1	2.1	2.1	0.275	2.1	2.1		
k_{DM} (10^{10} M^{-1} Hz)	1.4_5	1.6_5	1.8_0	2.1_0	3.1	2.3_5	2.6		
k_{MD} (10^6 Hz)	0.18	0.31	0.69	1.5_2	13	3.0	6.0		
k_D (10^6 Hz)	4.6_3	5.2_6	5.0_7	5.4_3	2.27	6.0_4	6.0		
k_{QD} (10^7 M^{-1} Hz)	4.1_4				840	7.2_0		8.8_3	10.5
q_{fM} (ab)					(1.0)[b]	0.28			
k_{fM} (10^6 Hz)					<2.75	5.9			
k_{im} (10^7 Hz)						1.5			
q_{fD} (abs)						0.18			
k_{fD} (10^6 Hz)						1.1			
k_{iD} (10^6 Hz)						5.0			

[a] Vapor phase data from ref 10. [b] Assumed value; see ref 10 and 18.

constants (in *n*-hexane solution) are very similar: i.e., $2.0 \pm 0.2 \times 10^7$ Hz.[29] For the rigid, bicyclic amines, 1-azabicyclo[3.3.3]-undecane (also known as ABCU or manxine), k_{fM} has a similar value: 2.1×10^7 Hz. For both ABCO and 1-AA, however, k_{fM} values are considerably smaller, i.e., 5.9×10^6 and 1.1×10^6 Hz, respectively. This may be a consequence of the fact that these cage amines are structurally prevented from achieving a planar configuration (with respect to the N atom) in their relaxed excited states.

It has been inferred from ESR studies that radical cations of these amines are also nonplanar.[30] These ionic species would, of course, represent the extreme case of electronic excitation. It is reasonable to assume that the acyclic and monocyclic amines cited above do, in fact, become planar in their relaxed lowest electronic state. The case of ABCU, with its k_f value comparable with those of the flexible amines is interesting. The ground state of the ABCU molecule is constrained by the three trimethylene bridges so that the N atom is considerably flattened relative to "unconstrained" amines;[31] e.g., the C-N-C bond angles are about 115° relative to ca. 109° for the flexible amines.

Unfortunately, because of the severe crowding of the $S_1 \leftarrow S_0$ and the $S_2 \leftarrow S_0$ transitions in the flexible amines, it is impossible to compare the k_{fM} values for the amines mentioned above with the respective integrated $S_1 \leftarrow S_0$ absorption spectra. Such an analysis has been performed for the only cage amines in the vapor phase.[18] From the data concerning the k_{fM} values of the flexible amines vis-a-vis the rigid ones, it appears that the transition moment integral (for emission, at least) is sensitive to the chromophore geometry. The lack of temperature dependence of k_{fM} for the cage amines suggests but does not totally support the possibility that it is the electronic (rather than vibrational) part of the transition moment integral which is sensitive to the amine structure.[32]

The difference in the k_{fM} values for 1-AA and ABCO (a factor of ca. 5.4) is not easily rationalized. Both cage amines possess similar structural arrangements about the N atom and significant differences in the C-N-C bond angles are not expected. From ESR studies of the radical cations, it has been deduced that $(1\text{-AA})\cdot^+$ is somewhat more planar (with respect to the N atom) vis-a-vis $(\text{ABCO})\cdot^+$. On the basis of the argument raised above concerning ABCU, it would be expected that k_{fM} be *larger* for 1-AA than for ABCO. This is not the case (see Tables II and III) and suggests that other factors than simply the configuration of the N atom must also affect the radiative transition probabilities in the saturated amines.

From the data contained in Table III, it can be seen that the value of k_{fM} for the cage amines increases by the factor of roughly 3 in going from the vapor phase to *n*-hexane solution. This effect appears to characterize the saturated amine excited state which presumably is largely Rydberg in nature (vide supra). The solvent medium also enhances the nonradiative relaxation rate(s) of the amine relative to the vapor state. It is not clear just what the nonradiative decay route is because neither (significant) photochemical activity nor phosphorescence is observed under any conditions (i.e., vapor or condensed phase, or low temperature). One might presume, then, that relaxation to the ground state proceeds via an internal conversion and that this process is enhanced by the presence of the solvent medium.

For both 1-AA and ABCO, the value of the excimer formation rate constant, k_{DM}, is observed to be consistent with that of a diffusion-controlled process. This is also the case for many aromatic excimer and exciplex forming molecules.[4,33]

Table IV. The Frequency Factors, Activation Parameters, and Binding Energies, B, of the 1-AA and ABCO Excimers (W and B (kcal/mol); A (Hz); and A_{DM} and A_{QD} (M^{-1} Hz))

Amine	A_M	W_M	A_{iD}	W_{iD}	A_{fD}	W_{fD}	A_{DM}	W_{DM}	A_{MD}	W_{MD}	A_{QD}	W_{QD}	B^a
1-AA	1.2×10^7	~0	1.4×10^6	~0	2.9×10^5	~0	1.4×10^{11}	1.2	1.2×10^{15}	11.4	$<10^7$	~0	10.2
ABCO	2.1×10^7	~0	4.9×10^7	1.4	1.1×10^6	~0	5.3×10^{11}	1.9	1.3×10^{16}	13.5	1.1×10^9	1.7	11.6

[a] $B = W_{MD} - W_{DM} = -\Delta H°$.

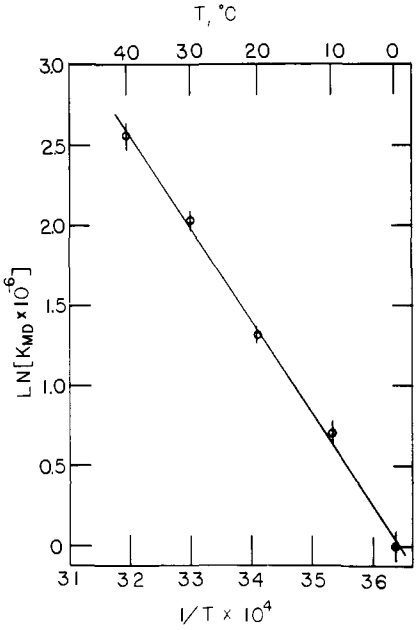

Figure 12. Plot of ln (k_{MD}) vs. $1/T$ for the 1-AA excimer.

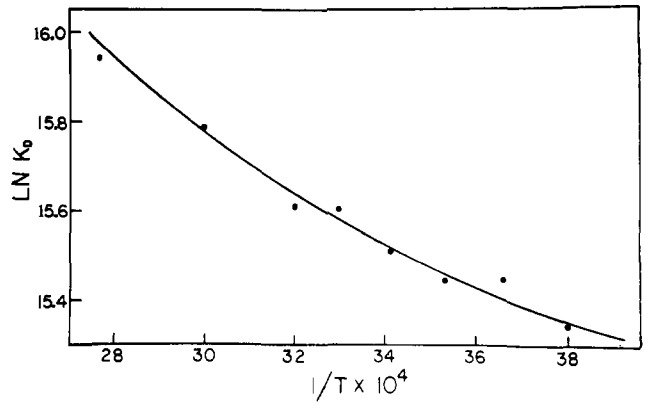

Figure 13. Plot of ln (k_D) vs. $1/T$ for the ABCO excimer.

Recently, Ware et al. have demonstrated the necessity of including the transient term ($t^{-1/2}$) in the analysis of the photokinetics of certain exciplexes.[33] For the 1-AA and ABCO excimers, satisfactory decay curve comparisons were achieved in convolution analyses without the inclusion of the $t^{-1/2}$ term to k_{DM}. This may be a result of the fact that in the study reported here, a rather low viscosity solvent medium (*n*-hexane) was used, and thus the diffusion coefficients of A and A* might be too large to give enough importance to the $t^{-1/2}$ term.[33,34]

The temperature dependence of k_{DM} for both 1-AA and ABCO (see Tables II-IV) is also consistent with a solvent-limiting process, i.e., W_{DM} is 1.2-1.9 kcal/mol. An Arrhenius plot of ln (T/η) for *n*-hexane furnishes a slope of ca. 2.3 kcal/mol. A direct relationship between the macroscopic solvent viscosity and a quenching constant (e.g., reaction efficiency), and also between their respective temperature dependencies, is not always expected; i.e., cage effects and the structural similarity of the solvent and solute must be taken into account.[35,36]

The fact that the excimer formation rate constants are diffusion controlled despite the fact that a specific orientation (or orientations) is (are) required for excimer stabilization can be rationalized by assuming that several collisions of A and A* can take place within a solvent cage (i.e., per encounter) during the A* lifetime. In contrast to this situation, k_{DM} measured in the vapor phase for ABCO indicates that excimer formation proceeds with a net efficiency of ca. 0.2.[10]

As is typical of the dissociation rate constants of many aromatic excimers and exciplexes, k_{MD} for the ABCO and 1-AA excimers are characterized by rather large preexponential factors, i.e., ~10^{15}-10^{16} (see Table IV). This implies that these excimers are tightly constructed and that the configurational requirements for stabilization are specific. The possible geometries of these saturated amine excimers will be commented on later.

The temperature dependence of k_{MD} for both ABCO and 1-AA is rather strong, as is to be expected from the steady-state estimates of the binding energies (vide supra). An Arrhenius plot of k_{MD} for the 1-AA excimer is shown in Figure 12 and provides a value for the dissociation activation energy, W_{MD}, of 11.4 kcal/mol. The frequency factor and activation energy for the ABCO excimer were obtained from the analogous plot of k_{MD} values and are also presented in Table IV.

Ware et al.[37,38] have presented data indicating that a correlation exists between log (A_{MD}) and W_{MD} both for excimers and exciplexes. In connection with exciplexes, it has been suggested that the foundation for this correlation lies in the similarity of the binding mechanism, i.e., in the force constants pertinent to exciplex[33] stabilization. It is interesting to note that the A_{MD} and W_{MD} values listed in Table IV for 1-AA and ABCO correlate fairly well with those presented in Figure 6 of ref 37 (which contains excimer as well as exciplex data). A more recent correlation of this type for exciplex systems only[38] shows that the saturated amine excimer activation parameters do not fit nearly as well, although it appears that the amines possess a similar isokinetic temperature: [$\Delta W_{MD}/R\Delta(\ln A_{MD})$]. From the data in Table IV, this is approximately 415 K (cf. 582 K from ref 37 and 475 K from ref 38). One must be cautious in assuming that such correlations imply similar binding mechanisms in the exciplexes (in which charge resonance is important, vide infra) vis-a-vis the excimers (both aromatic and saturated amines).

The data presented in Table III for the ABCO excimer reveal that k_D is slightly temperature dependent. An Arrhenius plot of these data, shown in Figure 13, is distinctly curved. Because k_D is equal to the sum of the excimer radiative and (total) nonradiative parts, k_{fD} and k_{iD}, the k_D data were analyzed using two simple assumptions: (1) k_{fD} is temperature independent and k_{iD} is temperature dependent, and (2) the opposite of (1). It was found that the k_D data could be analyzed so that either (1) or (2) could be satisfied: i.e., an Arrhenius plot of the data in which a constant was first subtracted from k_D was linear. From the data in Table III, the values of k_{iD} and k_{fD} are 5.0×10^6 Hz and 1.1×10^6 Hz, respectively, at 30 °C.

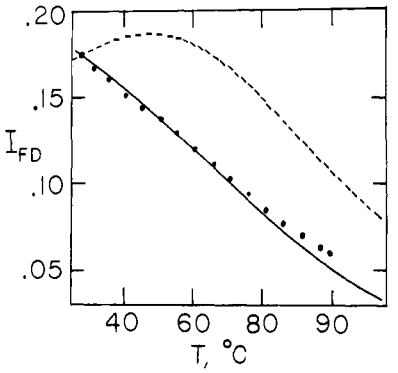

Figure 14. Plot of I_{fD} for the ABCO excimer vs. T (°C). (●) Experimental points; (—) calculated from (15) in which k_{fD} is constant and other rate constants are varied in conformity with the data in tables III and IV; (- - -) calculated from (15), but k_{iD} is constant and the other rate constants are varied as before (see text).

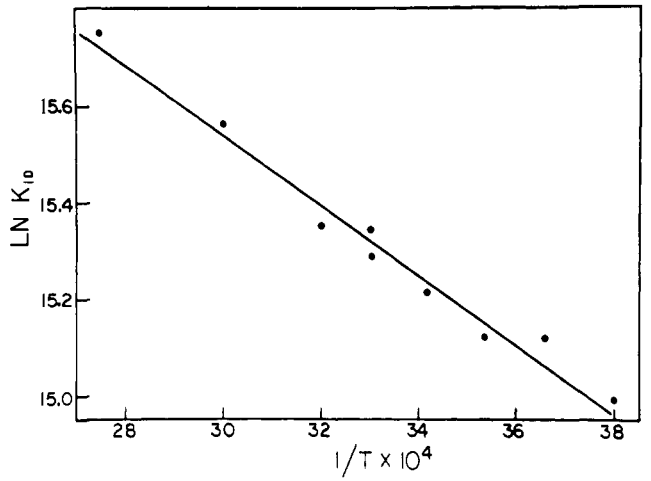

Figure 15. Plot of ln (k_{iD}) vs. $1/T$ for the ABCO excimer. k_{fD} is taken as 1.1×10^6 Hz and assumed to be independent of temperature.

In order to distinguish between cases (1) and (2), above, the temperature dependence of the steady-state excimer quantum intensity of ABCO (I_{fD}) was examined in more detail. In scheme 1 k_{iD} was taken as 5.0×10^6 Hz between 30 and 100 °C while in scheme 2 k_{fD} was assumed to be equal to 1.1×10^6 Hz over this temperature range. The results of these comparisons are depicted in Figure 14 in which I_{fD}, obtained from the following expression is plotted vs. T:

$$I_{fD} = \frac{k_{fD}/k_D}{1 + \dfrac{k_M(k_{MD} + k_D)}{k_D k_{DM} C}} \qquad (15)$$

where, of course, $k_D = k_{iD} + k_{fD}$.

In Figure 14, the solid line represents I_{fD} calculated from expression 15 in which k_{fD} is held constant (1.1×10^6 Hz), and the other rate constants are varied in accordance with the data in Tables III and IV, while the dashed curve pertains to the situation in which k_{iD} is constant (1.1×10^6 Hz) etc. The experimental points are clearly supportive of scheme (1). Values of k_{iD} were then obtained from the data in Table III and using $k_{fD} = 1.1 \times 10^6$ Hz. An Arrhenius plot of k_{iD} is shown in Figure 15 and is reasonably linear, having an activation energy (W_{iD}) of ca. 1.4 kcal/mol. Birks et al.[39] have reported that for the pyrene excimer, the temperature dependent component of the k_{iD} (which is assigned as an internal conversion) has an activation energy of ca. 2.3 kcal/mol in *cyclo*hexane. They also concluded that values of W_{iD} correlated with the activation

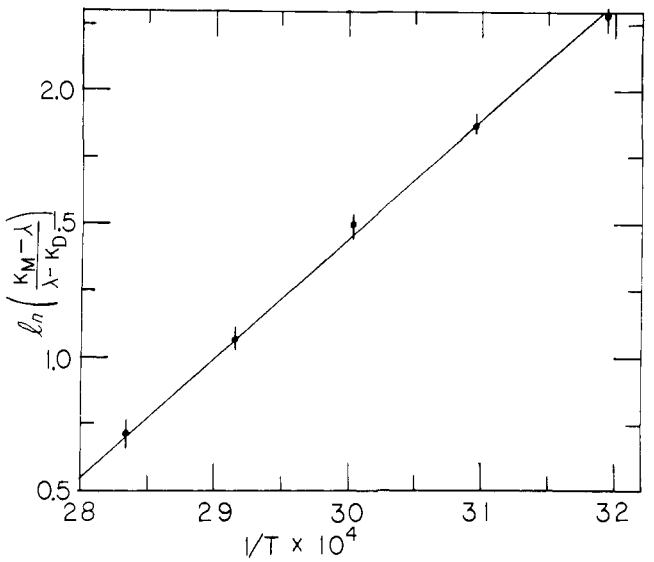

Figure 16. Plot of ln $[(k_M - \lambda)/(\lambda - k_D)]$ vs. $1/T$ for 1-AA (1.2×10^{-2} M in *n*-hexane). k_M and k_D are taken as 1.31×10^7 and 2.2×10^6 Hz, respectively.

energies to viscous flow of the solvent media used and that this radiationless process is facilitated by molecular motions which are largely impeded by the bulk medium.

Although W_{iD} for the ABCO excimer is somewhat smaller than the respective *n*-hexane viscosity parameter (vide supra), it should be pointed out that W_{DM} is also slightly smaller than $W_{T/\eta}$. Thus even presuming that W_{iD} represents some excimer vibrational mode (ca. 470 cm^{-1}) which induces radiationless deactivation, it need not necessarily follow that internal molecular distortion energy should correlate with the parameters associated with the macroscopic solvent viscosity.

High Temperature Behavior

It is well known that above a certain temperature (which depends both upon the binding energy of the excimer and also the values of k_M and k_D), the nonexponential decay curves usually observed for the monomer and excimer appear to be exponential. Thus both the monomer and excimer decay with common "lifetimes". Birks has shown that, kinetically, the decay constant, λ, observed in the high-temperature region can be represented as:[4]

$$\lambda = \frac{k_M + k_D k_{DM} C/k_{MD}}{1 + k_{DM} C/k_{MD}} \qquad (16)$$

This phenomenon is observed for the ABCO and 1-AA excimer systems above ca. 40 °C, which has been denoted above as T'. The mathematical (kinetic) requirements for this situation are $k_{MD} \gg k_D$ and $k_{DM}C \gg k_M$ to which Ware et al.[25] add the condition $k_{MD} + k_{DM}C \gg [2(k_{MD} - k_{DM}C)(k_D - k_M)]^{1/2}$

Equation 16 can also be expressed as

$$(K_e)_0 C = \frac{k_M - \lambda}{\lambda - k_D} \qquad (17)$$

where $(K_e)_0$ is the molar equilibrium constant pertaining to excimer formation. Accordingly, an Arrhenius plot of the right-hand-side of (17) can be used to determine $\Delta H°$ and $\Delta S°$, assuming that both k_M and k_D are temperature independent. Such an evaluation has been performed for the 1-AA and ABCO excimers using the excimer fluorescence decay data for these amines at high concentrations ($>10^{-3}$ M) and at temperatures between ca. 50 and 100 °C. An Arrhenius plot of the data obtained for the 1-AA excimer is depicted in Figure 16, where the values of k_M and k_D used are 1.31×10^7 and 2.2

Table V. Thermodynamic Characteristics of the 1-AA and ABCO Excimer Formation. $\Delta G°$ and $\Delta H°$ Are in Units of kcal/mol, and $\Delta S°$ Is in eu

Amine excimer	$(K_e)_0$	$-\Delta G°$	$-\Delta H°$	$-\Delta S°$
ABCO	1.71×10^4	5.85	11.6	19
ABCO (vapor)[a]	$9.7_6 \times 10^3$ [b]	5.5[b]	11.6[c]	20
1-AA	$3.9_3 \times 10^3$	5.0	10.2	17

[a] Data from ref 10. [b] Value reflects the vapor phase standard state of 1 atm. [c] Value assumed to be the same as that in *n*-hexane solution.

$\times 10^6$ Hz, respectively. The plot in Figure 16 furnishes values of ΔH and ΔS of -9.0 kcal/mol and -15 eu, respectively, which are consistent with the activation and thermodynamic parameters listed in Tables IV and V. It should be pointed out that $\Delta H°$ and $\Delta S°$ obtained for 1-AA using the method described above are rather sensitive to the particular value of k_D used. For example, if k_D is taken as 2.0×10^6, a linear Arrhenius plot is produced which yields a value of $\Delta H°$ of ca. -8.8 kcal/mol. Errors become very large at low temperatures (ca. 40 °C where $\lambda \rightarrow k_D$) and also at higher temperatures where λ can approach k_M. This latter problem did not arise in the case of 1-AA. The reasonable linearity of the ln $[(k_M - \lambda)/(\lambda - k_D)]$ plots implies that for 1-AA both k_M and k_D are either temperature independent or have only very small dependencies.

For ABCO, where k_D has been shown to be slightly temperature dependent, this Arrhenius plot was also linear and gave $\Delta H°$ and $\Delta S°$ values which agree well with the data listed in Tables IV and V; namely -11.1 kcal/mol and -16.4 eu, respectively.

It is interesting to consider the possibility of utilizing the Arrhenius plot of eq 17 in elucidating either binding energies and/or k_D values for exciplexes and also for weakly bound excimers for which the high-temperature region commences far below ambient temperatures. Presumably for such systems k_M is readily obtained. It may also be constructive to use this approach in studying intramolecular excimers and exciplexes in which monomer emission may not be observable except at very low temperatures.

Structure of the Saturated Amine Excimer

One of the central questions to be answered concerns the configuration of the saturated amine excimers described in this paper. Although the fluorescence properties of a rather large variety of saturated tertiary amines have been examined, including many acyclic, monocyclic, and bicyclic amines, only the three compounds described here unequivocally undergo intermolecular excimer formation. Thus, even if in other systems where self-quenching occurs and excimer formation might take place, the excimer must be very weakly bound, or otherwise be characterized by an extremely large deactivation rate (relative to the excimers described herein). The criterion for excimer formation and stabilization cannot simply involve the bicyclic nature of these N-bridgehead systems because certain analogous amines, e.g., a derivative of 1-azabicyclo[3.3.1]nonane, 1-azabicyclo[3.3.3]undecane (ABCU), and 1,4-diazabicyclo[2.2.2]octane (DABCO), fail to excimerize. The latter two cases will be discussed below.

As mentioned above, the rather large negative entropies of formation for the 1-AA and ABCO excimers (ca. -17 and -19 eu, respectively) imply a rather tight and discrete configuration. The fact that 4-Me-ABCO excimerizes strongly suggests that the methine hydrogen plays no role in excimer stabilization and that therefore the excimer almost certainly does not form in a "head-to-tail" fashion in which the C_3 symmetry axes of the molecules are collinear. Excimer formation and the similar thermodynamic properties of 1-AA (vis-a-vis ABCO) also support this idea.

A logical configuration to consider for the excimers is the one in which the amines are arranged in a "head-to-head" manner (structure I). According to this picture, the two N

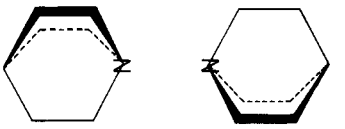

I

atoms face each other and the molecules are oriented along the same symmetry axis, presumably in such a way so that the bridge systems of the two amines are staggered. This model would apply to all three of the excimer-forming amines. It is also possible that the excimer is not coaxially oriented, but arranged so that one of the N–C bonds of an amine is antiparallel with respect to an N–C bond of its partner as suggested in structure II. Although there exist other logically possible

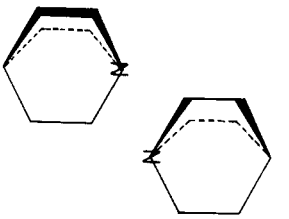

II

structures, the two described above appear to be more intuitively reasonable.

On the basis of the thermodynamic and kinetic data alone, it is not possible, of course, to assign or speculate about a particular structure for the excimer. Unlike the case of pyrene, in which the fluorescence properties of the crystal were important in proposing the excimer structure, the respective crystal emission spectra of ABCO and 1-AA provide no definitive information. The crystal emission spectra of both amines are broad and very red-shifted relative to the monomer emission bands observed in solution; the fluorescence, in fact, appears as a violet emission. The crystal structure of ABCO is reported to be face-centered cubic with a unit cell length of ca. 9 Å.[40,41] The ABCO molecules are presumed to be oriented in parallel arrangements (i.e., head-to-tail) in which the "directionality" alternates from row to row. X-ray diffraction studies of the ABCO single crystal appear not to have been reported. It is not clear, then, that the limited information available concerning the ABCO crystal structure can be used to support or even infer the structure of the excimer in the vapor or solution phase. Perhaps the violet emission observed from the ABCO and 1-AA crystals is a consequence of site defects or surface discontinuities.

Nature of the Binding Mechanism

The binding forces in excimers and exciplexes are usually considered to arise from two types of interactions: excitation dipole–dipole (exciton resonance) and electrostatic (charge resonance).[4,5] It is very interesting to consider what the bonding mechanism might be for the saturated amine excimers, and whether the energetics of excimer formation can be rationalized within the framework which is usually applied to the aromatic excimers.

In considering purely exciton resonance stabilization, one

must know the electronic transition origins and their respective oscillator strengths. This information is available for ABCO and 1-AA in the vapor phase, although the $S_1 \leftarrow S_0$ transition for the latter amine has not been measured quantitatively (see Table I and ref 15). The three electronic transitions which are observed for ABCO (below its ionization energy) are weakly to moderately allowed. The oscillator strengths (f values) of the first two transitions for this amine are about 0.003 and 0.06, respectively.[15] The third transition rests upon an underlying continuum making the measurement of f unreliable. The f value for the $S_2 \leftarrow S_0$ transition of 1-AA (shown in Figure 2 of ref 42) is ca. 0.04 which is similar to that of the respective ABCO transition. Simple exciton resonance calculations based on the f values and transition origins of ABCO show that neither electronic transition is strongly enough allowed to provide the required stabilization (i.e., the measured binding energy) at any reasonable intermolecular separation. Thus, taken alone, exciton resonance appears to be inadequate in rationalizing the excimer binding mechanism.

In considering a purely Coulombic interaction between the electronically excited and ground-state species (charge resonance), the stabilization energy (assuming radical cation and radical anion wavefunctions) is expressed as

$$W_R = I - A - C(r)$$

where I and A are, respectively, the ionization potential and electron affinity of the amine, and $C(r)$ is the coulombic attraction of the radical ions (i.e., $e^2/\epsilon r$), r being the separation between the (point) charges. Based on the known ionization potentials of the amines (8.02 and 7.94 eV for ABCO and 1-AA, respectively),[19] it appears that one might be able to rationalize the stabilization of the amine excimers on the basis of a simple charge resonance model. However, in order to account quantitatively for the observed binding energies of ca. 10 kcal/mol (see Table IV), and assuming a molecular separation of 2.5 Å (e.g., between N atoms in structure I above), the electron affinities of these compounds would have to be $>+1.7$ eV which seems to be unreasonably large.

Thus neither the exciton resonance nor the charge resonance models, considered alone, seems to be adequate in accounting for the stabilization in the saturated amine excimers. It is possible that, like the situation in the aromatic excimers (e.g., pyrene[5]) configuration interaction between the eigenstates derived from these models might result in excimer wavefunctions whose eigenvalues are more consistent with the experimental data.

Irrespective of which model (or models) is (are) used to compose the excimer wavefunctions and eigenvalues, it is crucial that the treatment adequately account for the rather unique specificity which governs saturated amine excimer formation. As mentioned above, no other type of saturated tertiary amine appears to undergo excimer formation, and these include certain analogous compounds such as DABCO and ABCU The nonexcimerization of DABCO can be rationalized on the basis of the fact that this amine is a ground-state coupled system and possesses, therefore, different spectroscopic and photophysical properties relative to monoamines.[19b,43-46] ABCU is also rather different from other monoamines because the constraints imposed by the trimethylene bridges cause the partial flattening of the N atom vis-a-vis the three α-C atoms. The C-N-C bond angle is reported to be ca. 115 °C.[31] The possible importance of the C-N-C bond angle, as well as structural rigidity, will be discussed below.

Several INDO calculations were performed on a series of amine pairs in order to elucidate which structural parameters were important in affecting excimer stabilization. The model used for the excited-state amine was the radical cation, a species which represents the limit of electronic excitation for Rydberg states. These calculations indicate that there is a substantial stabilization for a neutral ABCO molecule in association with the ABCO radical cation (relative to the two neutral molecules) at distances less than about 3 Å. The geometry chosen for this calculation is that indicated in structure I above.

Similar calculations were performed for a pair of trimethylamine molecules, one neutral and the other as the radical cation: In case I, the radical was given a planar configuration which is consistent with its known structure as well as that of the excited state,[13,30] and the neutral molecule was kept pyramidal. In case II, both species were kept in a pyramidal arrangement, and in case III, both were constrained to be planar. In each of the three cases, stabilization resulted (relative to the respective pair of neutral molecules), but the magnitude of the stabilization increased in the sequence: case II > case I > case III. It should be realized that in these calculations, the stabilization is to be interpreted qualitatively because the energetics pertaining to the radical cation vis-a-vis the electronically excited states are expected to be different. It is assumed, however, that the relative differences in stabilization energy are significant.

Thus, these calculations suggest that it is the ability of the N atom to avoid approaching polarity with respect to the three α-carbon atoms in the excited state which is important in determining excimer stability. This hypothesis can be used to rationalize why ABCU, having a *ground*-state C-N-C bond angle of about 115° (which is probably larger in the excited state) fails to excimerize. This rationalization can be likewise applied to the flexible nonexcimerizing amines which are planar, or nearly planar in their excited states. The involvement of some loosely bound excimer in the mechanism of the self-quenching of these amines is, nevertheless, a possibility.[47]

There is one striking, common structural feature which all three of the excimerizing amines possess. Each of the three α-β C-C bonds is directed in parallel orientation with respect to the N n orbital. It is this sort of orbital arrangement which is responsible for the "through-bound" ground-state coupling in DABCO.[43,44] Conceivably, it is this unique configuration of orbitals in ABCO, 1-AA, and 4-Me-ABCO which represents the criterion for excimer formation in the saturated amines. It has been proposed by Hoffmann et al. that the orbital coupling in the transition state of the Grob fragmentation reaction is predicated on a 1-4 interaction in which the N n orbital and the α-β C-C σ bonds interact.[48] This electronic coupling, then, activates the leaving group in the 4 position, and thus facilitates the fragmentation.

If the special structural disposition of the N and α-β C atoms described above for ABCO and 1-AA were indeed the key factor in promoting excimer stabilization, then one would expect some spectroscopic property of these amines to reflect, accordingly, this situation. Another way of viewing this would be to propose that the aliphatic framework of the cage amine acts as a good electron hole vis-a-vis electronic excitation and that a large(er) dipole reversal results consequent to electronic excitation, relative to other amines. If this were actually the case, one would expect that the electronic transition strengths of ABCO and 1-AA would be larger than those of the nonexcimerizing amines. As mentioned above, this is not the case. In fact, there does not seem to be any particularly unusual spectroscopic characteristic of these amines. One (seemingly remote) possibility is that the electron affinities of these cage amines are abnormally larger than those of other saturated tertiary amines.

If the INDO calculations described above are correct in providing some pathway to understanding the structural requirements, at least, for excimer formation, then one would predict that compounds such as 1-azabicyclo[2.2.1]heptane, and other such analogues, whose C-N-C bond angles are constrained by the cage system to be less than ca. 109° should

also undergo excimer formation. In such compounds, of course, the collinear arrangement of the N n orbital and the α-β C-C bonds becomes gradually diminished. Investigations in this area are currently being pursued.

Photochemical Studies

Some experiments were performed in order to investigate the consequence of excimer formation on the photochemical stability of the saturated amines. Triethylamine (TEA) and ABCO were both photolyzed in *n*-hexane solutions, at various concentrations using a 500-W Hg lamp. Degassed solutions of the amines in Suprasil tubes were exposed to the unfiltered lamp for periods proportional to the concentrations of the amines. The disappearance of the starting amine was determined using standard gas chromatographic techniques.

Both amines are surprisingly photostable, having disappearance fractions of not more than 0.1 for 50 h of irradiation. For TEA, the disappearance was ca. 3–4% irrespective of concentration (10^{-4}–10^{-2} M), while that for ABCO appeared to increase from ca. 3% to ca. 10% over the same concentration range and under identical irradiation conditions. These results suggest that the excimer is more photoreactive than the monomer. No other component was observable via VPC consequent to photolysis; however, because of the large amount of starting material present in these analyses, trace amounts of other components could have been masked. In the more concentrated solutions, irradiation resulted in the production of turbid solutions, presumably due to polymer formation.

Experimental Section

Materials. ABCO was obtained from Aldrich Chemical Co. as the hydrochloride. The free base was liberated by combining very concentrated aqueous solutions of ABCO·HCl and NaOH. The solid base was then filtered and repeatedly sublimed under high vacuum. The first sublimation was usually carried out from a mixture of the base and anhydrous BaO_2; ABCO mp, 160 °C (sealed tube). 1-AA was provided through the courtesy of Professor W. N. Speckamp. The free base was judged to be adequate for use without further purification on the basis of quantitative absorption spectra, both in the vapor phase and in *n*-hexane solution (see Table I). 4-MA was kindly furnished by Professor C. A. Grob as the hydroperchlorate salt. The free base was liberated using the procedure described above for ABCO. The amine, an oil, wa extracted with a small amount of 2-methylbutane and then retrieved (and dried) via preparative GLC using a Carbowax and KOH-coated Chromosorb P column. All investigations reported in this paper were carried out in *n*-hexane solution. This solvent (Matheson Spectroquality) was found to be adequate for most measurements without further purification. Certain experiments (e.g., those involving dilute solutions) were more sensitive to background emission, and in these cases, the solvent was purified by being passed through a $AgNO_3$·Al_2O_3 column and then distilled. Toluene was distilled immediately prior to use, and α,α'-binaphthyl (Eastman) was sublimed just prior to use.

Emission Spectra and Quantum Yield Measurements. Fluorescence spectra were obtained using a conventional dc fluorimeter described elsewhere.[46] For most experiments, the 232-nm Hg line was isolated from a 200-W Hg–Xe lamp. The excitation band-pass was less than 3nm, and the emission band-pass was usually 2 nm. Emission spectra reported here are uncorrected. Quantum yield measurements of the amine monomer fluorescence utilized toluene (in *n*-hexane) as the absolute standard. A value of ϕ_f (toluene) of 0.14 was used. This is the Berlman value[50] modified by Birks.[51] For the amine excimer fluorescence, α,α'-binaphthyl was chosen as the standard because of the favorable coincidence of its fluorescence spectrum vis-a-vis those of the amine excimers. Because of good spectral overlap of the fluorescence standards with their respective amine emission bands,these spectra were not corrected in the quantum yield determinations. Reference and standard solutions were designed such that their respective optical densities at the excitation wavelengths used (238 nm for monomer and 249 nm for excimer) were within about 10% of each other. This was done in order to minimize possible discrepancies arising from optical (geometrical) differences between reference and unknown. In all cases, the observed fluorescence intensities were corrected with respect to the amount of light absorbed.

For the measurements of q_{fM} for 1-AA and ABCO, dilute solutions of the amines were used (ca. 1×10^{-4} M). Although excimer formation is relatively unimportant in these solutions (as evidenced by the apparent absence of excimer emission), excimer formation and dissociation back into monomer was nevertheless taken into account by using the following relation:

$$q_{fM} = I_{fM}\left[1 + \frac{k_D k_{DM} C}{k_M(k_D + k_{MD})}\right]$$

where I_{fM} is the (observed) fluorescence intensity of the monomer, and q_{fM} is the intrinsic quantum yield of the monomer. Values of the rate constants were furnished from measurements at ambient temperature. This correction, both for 1-AA and ABCO was ca. 10%.

For the excimer quantum yield (q_{fD}) measurements, concentrated solutions (ca. 1×10^{-2} M) of the amines were used. Using the analogous procedure to that described above, the observed fluorescence intensities (I_{fD}) were corrected for dissociation into monomer (and, in the case of ABCO, ground-state quenching). These adjustments utilize the following relation:

$$q_{fD} = I_{fD}\left[1 \cdot \frac{k_M(k_D + k_{MD})}{k_D k_{DM} C}\right]$$

The estimated errors in the measured quantum yields are 10% for monomer and about 20% for excimer.

Fluorescence Lifetime Measurements. The time-correlated single photon method was used; the technique, as well as the particular apparatus employed, has been described elsewhere.[18,49] For monomer measurements, a 2789 Å interference filter (Corion Instrument Corp.) was used, and for excimer measurements one (or sometimes two) Corning Glass 0-52 filter was used. The flash lamp was a thyratron-driven (12–20 kHz), low pressure (0.5 atm) D_2 discharge constructed from Pt electrodes and which was run at about 7 kV. The fwhm was ca. 2.5 ns, and the $1/e$ time was about 0.8 ns for nearly three decades of decay. For many measurements, a small, high-voltage ceramic disk capacitor (10–20 pF) was added to the firing electrode in order to intensify (and slightly broaden) the main pulse in relation to the long-lived tail. This had the distinct advantage of reducing the distortion otherwise observed in fluorescence decay curves at long times (> ca. 500 ns).

In all cases, the monomer and excimer decay curves were analyzed by the convolute-and-compare method using a computer-interfaced X-Y plotter. This rocedure was crucial in assigning precise values to the short-lived decay constant (λ_2) and relative amplitude of the monomer decay curve. Data acquisition times were kept long enough in order to enable as precise measurements of the decay curve parameters λ_1, λ_2, and A as possible. In the most favorable cases, λ_1 and λ_2 could be measured with less than ca. 1% accuracy. The accuracy attainable in the A values depended strongly upon the particular temperature and amine concentration.

Temperature Control. Most kinetic and steady-state measurements were carried out using a jacketed fluorescence cell (Hellma Cells, Inc.) which was attached via a graded seal to a degassing bulb and other associated glassware. Other measurements employed the usual square fluorescence cell which was placed in a machined-out brass block. For high-temperature experiments, ethylene glycol was circulated through the jacketed cell (or the brass block) using a Haake-Ultra-Thermostat. For the low-temperature measurements, a Precision Scientific refrigerated probe was used in conjunction with the temperature bath, in which case methanol was used as the circulating fluid. Temperature accuracy and control was about 0.1–0.5 °C.

Acknowledgment. The authors are grateful to the National Science Foundation for its support of this research. The donors of the Petroleum Research Fund, administered by the American Chemical Society, are also acknowledged for partial support. Professor K. Weiss and Mr. E. Reid were very helpful in the performance of the INDO calculations. Professors C. A. Grob and W. N. Speckamp are gratefully thanked for their cooperation in providing samples of 4-Me-ABCO and 1-AA, respectively.

References and Notes

(1) Alfred P. Sloan Research Fellow.
(2) Ecole Superieure de Physique et de Chimie Industrielles de la Ville de Paris.
(3) Portions of this material constitute partial fulfillment of the Ph.D. degree of R.J.S. (New York University).
(4) J. B. Birks, "Photophysics of Aromatic Molecules", Wiley-Interscience, London, 1970, pp 301–371.
(5) J. B. Birks in "Progress in Reaction Kinetics", Vol. 5, G. Porter, Ed., Pergamon Press, Oxford, 1970.
(6) T. Vala, Jr., I. H. Hillier, S. A. Rice, and J. Jortner, *J. Chem. Phys.*, **44**, 23 (1966).
(7) H. Lami and G. Laustriat, *J. Chem. Phys.*, **48**, 1832 (1968).
(8) J. Eisinger, M. Guron, R. G. Shulman, and T. Yamane, *Proc. Natl. Acad. Sci. U.S.A.*, **55**, 1015 (1966).
(9) A. M. Halpern and E. Maratos, *J. Am. Chem. Soc.*, **84**, 8273 (1972).
(10) A. M. Halpern, *J. Am. Chem. Soc.*, **96**, 4392 (1974).
(11) Excimer formation in the noble gases is a well-known phenomenon; see J. B. Birks, *Rep. Prog. Phys.*, **38**, 903 (1975).
(12) A. M. Halpern and P. P. Chan, *J. Am. Chem. Soc.*, **97**, 2971 (1975).
(13) M. B. Robin, "Higher Excited States of Polyatomic Molecules", Vol. 1, Academic Press, New York, N.Y., 1974, pp 208–229.
(14) See ref 13, pp 8–31
(15) The electronic absorption spectrum of ABCO has been described by A. M. Halpern, J. L. Roebber, and K. Weiss, *J. Chem. Phys.*, **49**, 1348 (1968).
(16) A portion of the electronic absorption spectrum of 1-AA has been described by A. M. Halpern, *Mol. Photochem.*, **5**, 517 (1973); see ref 19.
(17) N. J. Leonard and D. M. Locke, *J. Am. Chem. Soc.*, **77**, 437 (1955).
(18) A. M. Halpern, *J. Am. Chem. Soc.*, **96**, 7655 (1974).
(19) Consistent with this idea, the vertical ionization potential of 1-AA is slightly lower than that of ABCO: (i.e., 7.94 eV vis-a-vis 8.02 eV): (a) C. Worrell, J. W. Verhoeven, and W. N. Speckamp, *Tetrahedron*, **30**, 3525 (1974); (b) P. Bischof, J. A. Hashmall, E. Heilbronner, and V. Hornung, *Tetrahedron Lett.*, **46**, 4025 (1969).
(20) Reference 13, p 220.
(21) A. M. Halpern and D. K. Wong, *Chem. Phys. Lett.*, **37**, 416 (1976).
(22) The radiative rate constants of the monomer and excimer are usually assumed to be independent of temperature; see J. B. Birks, A. J. H. Alwattar, and M. D. Lumb, *Chem. Phys. Lett.*, **11**, 89 (1971), and references cited therein.
(23) B. Stevens and M. I. Ban, *Trans. Faraday Soc.*, **60**, 1515 (1964); B. K. Selinger, *Mol. Photochem.*, **1**, 371 (1969); R. J. McDonald and B. K. Selinger, *ibid.*, **3**, 99 (1971).
(24) G. E. Johnson, *J. Chem. Phys.*, **61**, 3002 (1974).
(25) W. R. Ware, D. Watt, and J. D. Holmes, *J. Am. Chem. Soc.*, **96**, 7853 (1974).
(26) This case seems to apply to most aromatic excimers and certainly pertains to the saturated amine excimers.
(27) W_{MD}, the activation energy for excimer dissociation, usually correlates with the binding energy because formation activation energies are usually solvent dependent and smaller than W_{MD} values.
(28) This is probably a consequence of error correlations in the $\lambda_{1,2}$ values.
(29) A. M. Halpern, D. K. Wong, and A. L. Lyons, Jr., unpublished data.
(30) W. C. Danen and R. C. Richard, *J. Am. Chem. Soc.*, **97**, 2303 (1975).
(31) A. H.-J. Wang, R. J. Missavage, S. R. Byrn, and I. C. Paul, *J. Am. Chem. Soc.*, **94**, 7100 (1972).
(32) Vibronic coupling affected via a high-frequency mode would give rise to a very small temperature dependence.
(33) W. R. Ware et al., Abstracts of VIII International Conference on Photochemistry, Edmonton, Canada, August 1975, and private communication.
(34) W. R. Ware and T. Nemzek, *J. Chem. Phys.*, **62**, 477 (1975).
(35) A. H. Alwattar, M. D. Lumb, and J. B. Birks in "Organic Molecular Photophysics", Vol. I, J. B. Birks, Ed., Wiley, London, 1973.
(36) A. Yekta and N. J. Turro, *Chem. Phys. Lett.*, **17**, 31 (1972).
(37) C. Lewis and W. R. Ware, *Mol. Photochem.*, **5**, 261 (1973).
(38) M.-H. Hui and W. R. Ware, *J. Am. Chem. Soc.*, **98**, 4706 (1976).
(39) J. B. Birks, A. J. H. Alwattar, and M. D. Lumb, *Chem. Phys. Lett.*, **11**, 89 (1971).
(40) P. Brüesch, *Spectrochim. Acta*, **22**, 877 (1966).
(41) P. Brüesch and Hs. H. Günthard, fiSpectrochim. Acta, **22**, 877 (1966).
(42) A. M. Halpern, *Mol. Photochem.*, **5**, 517 (1973).
(43) R. Hoffmann, A. Imamura, and J. W. Hehre, *J. Am. Chem. Soc.*, **90**, 1499 (1968).
(44) E. Heilbronner and K. A. Muszkat, *J. Am. Chem. Soc.*, **92**, 3818 (1970).
(45) A. M. Halpern, *Chem. Phys. Lett.*, **6**, 296 (1970).
(46) A. M. Halpern and R. M. Danziger, *Chem. Phys. Lett.*, **16**, 72 (1972).
(47) A. M. Halpern, D. K. Wong, and B. R. Ramachandran, unpublished results.
(48) R. Gleiter, W.-D. Stoner, and R. Hoffmann, *Helv. Chim. Acta*, **55**, 893 (1972).
(49) C. Lewis, W. R. Ware, L. J. Doemeny, and T. M. Nemzek, *Rev. Sci. Instrum.*, **44**, 107 (1973).
(50) I. B. Berlman, "Handbook of Fluorescence Spectra of Aromatic Molecules", Academic Press, New York, N.Y., 1965.
(51) Reference 4, pp 103–105.

A One-Carbon Homologation of Carbonyl Compounds to Carboxylic Acids, Esters, and Amides

Stephen E. Dinizo, Robert W. Freerksen, W. Edward Pabst, and David S. Watt*

Contribution from the Department of Chemistry, University of Colorado, Boulder, Colorado 80309.

Received May 14, 1976

Abstract: An efficient sequence for the one-carbon homologation of aldehydes and ketones to carboxylic acids **2**, esters **3**, and amides **4** involves (1) the Horner–Emmons modification of the Wittig reaction using diethyl *tert*-butoxy(cyano)methylphosphonate $(EtO)_2POCH(CN)O$-*t*-Bu to afford α-*tert*-butoxyacrylonitriles **15**, (2) the cleavage of the *tert*-butyl ether in **15** using zinc chloride in refluxing acetic anhydride to afford α-acetoxyacrylonitriles **16**, and (3) the hydroxide, alkoxide, or amine solvolysis of **16** to afford **2**, **3**, or **4**, respectively, in 57–88% overall yield from the carbonyl compounds.

We have sought to develop useful methodology for the one-carbon homologation of carbonyl compounds **1** to carboxylic acids **2**, esters **3**, and amides **4**. To achieve this versatility, we required the generation of a transitory acyl intermediate capable of intercepting various nucleophiles to form the desired acyl derivatives. We now wish to report an efficient solution to this problem which relies on the liberation of a masked acyl cyanide.[1]

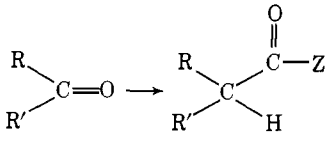

1 **2**, Z = OH; **3**, Z = OR″; **4**, Z = NR″$_2$

Available methodology for the transformation of carbonyl compounds **1** to carboxylic acids **2** has relied on the intermediacy of (a) cyanohydrins[2] **5** (Z = OH), (b) nitriles[3] **5** (Z = H), (c) ketene thioacetals[4] **6** (Z, Z′ = SCH_3, SC_6H_5, or $S(CH_2)_3S$), (d) α,β-unsaturated sulfones[5] **6** (Z = $SO_2C_6H_5$ or $SO_2C_6H_4$-*p*-CH_3; Z′ = NHCHO), (e) α,β-unsaturated phosphonates[6] **6** (Z = $PO(OC_2H_5)_2$; Z′ = $N(CH_3)_2$), (f) enol